BMC Biochemistry

Research article

Probing substrate binding to Metallo-β-Lactamase L1 from *Stenotrophomonas maltophilia* by using site-directed mutagenesis

Anne L Carenbauer, James D Garrity, Gopal Periyannan, Robert B Yates and Michael W Crowder*

Address: Department of Chemistry and Biochemistry, Miami University, Oxford, OH, USA

E-mail: Anne L Carenbauer - sutsong@yahoo.com; James D Garrity - garritjd@po.muohio.edu; Gopal Periyannan - periyag1@po.muohio.edu; Robert B Yates - yatesrb@po.muohio.edu; Michael W Crowder* - crowdemw@muohio.edu

*Corresponding author

Published: 13 February 2002

BMC Biochemistry 2002, **3**:4

Received: 6 November 2001
Accepted: 13 February 2002

This article is available from: http://www.biomedcentral.com/1471-2091/3/4

Abstract

Background: The metallo-β-lactamases are Zn(II)-containing enzymes that hydrolyze the β-lactam bond in penicillins, cephalosporins, and carbapenems and are involved in bacterial antibiotic resistance. There are at least 20 distinct organisms that produce a metallo-β-lactamase, and these enzymes have been extensively studied using X-ray crystallographic, computational, kinetic, and inhibition studies; however, much is still unknown about how substrates bind and the catalytic mechanism. In an effort to probe substrate binding to metallo-β-lactamase L1 from *Stenotrophomonas maltophilia,* nine site-directed mutants of L1 were prepared and characterized using metal analyses, CD spectroscopy, and pre-steady state and steady state kinetics.

Results: Site-directed mutations were generated of amino acids previously predicted to be important in substrate binding. Steady-state kinetic studies using the mutant enzymes and 9 different substrates demonstrated varying K_m and k_{cat} values for the different enzymes and substrates and that no direct correlation between K_m and the effect of the mutation on substrate binding could be drawn. Stopped-flow fluorescence studies using nitrocefin as the substrate showed that only the S224D and Y228A mutants exhibited weaker nitrocefin binding.

Conclusions: The data presented herein indicate that Ser224, Ile164, Phe158, Tyr228, and Asn233 are not essential for tight binding of substrate to metallo-β-lactamase L1. The results in this work also show that K_m values are not reliable for showing substrate binding, and there is no correlation between substrate binding and the amount of reaction intermediate formed during the reaction. This work represents the first experimental testing of one of the computational models of the metallo-β-lactamases.

Background

The overuse of antibiotics in the clinic and for agricultural uses has resulted in a tremendous selective pressure for antibiotic resistant bacteria. These bacteria become resistant by a number of mechanisms, such as producing enzymes that hydrolyze or inactivate the antibiotics,

producing efflux pumps that transport the antibiotic out of the cell, or modifying their cell wall components so they no longer bind effectively to the antibiotics [1–3]. The most common, least expensive, and effective antibiotics are the β-lactam containing antibiotics, such as the penicillins, cephalosporins, and carbapenems [2,4,5]. These antibiotics are mechanism-based inhibitors of transpeptidase, a bacterial enzyme required for the production of a strong viable cell wall [6,7]. In response to the widespread use of β-lactam containing antibiotics, bacteria have acquired the ability to produce β-lactamases, which are enzymes that hydrolyze and inactivate β-lactam containing antibiotics. There are over 300 distinct β-lactamases known, and these enzymes have been grouped by a number of classification schemes [8–15]. For example, Bush has developed a scheme, based on the enzymes' molecular properties, that has four distinct β-lactamase groups [10,15]. One of the more alarming groups are the Bush group 3 enzymes, which are Zn(II) dependent enzymes that hydrolyze nearly all known β-lactam containing antibiotics and for which there are no or very few known clinical inhibitors [9,14,16–19]. The metallo-β-lactamases have been further divided by Bush into subgroups based on amino acid sequence identity: the Ba enzymes share a >23% sequence identity, require 2 Zn(II) ions for full activity, prefer penicillins and cephalosporins as substrates, and are represented by metallo-β-lactamase CcrA from *Bacteroides fragilis*, the Bb enzymes share a 11% sequence identity with the Ba enzymes, require only 1 Zn(II) ion for full activity, prefer carbapenems as substrates, and are represented by the metallo-β-lactamase imiS from *Aeromonas sobria*, and the Bc enzymes have only 9 conserved residues with the other metallo-β-lactamases, require 2 Zn(II) ions for activity, contain a different metal binding motif than the other metallo-β-lactamases, prefer penicillins as substrates, and are represented by the metallo-β-lactamase L1 from *Stenotrophomonas maltophilia*[9]. A similar grouping scheme (B1, B2, and B3) based on structural properties of the metallo-β-lactamases has recently been offered [41]. The diversity of the group 3 β-lactamases is best exemplified by the enzymes' vastly differing efficacies towards non-clinical inhibitors; these differences predict that one inhibitor may not inhibit all metallo-β-lactamases [18,20–29]. To combat this problem, we are characterizing a metallo-β-lactamase from each of the subgroups in an effort to identify a common structural or mechanistic aspect of the enzymes that can be targeted for the generation of an inhibitor. It is hoped that this inhibitor, when given in combination with an existing antibiotic, will prove to be an effective therapy against bacteria that produce a metallo-β-lactamase. This work describes our efforts on metallo-β-lactamase L1 from *S. maltophilia*.

S. maltophilia is an important pathogen in nosocomial infections of immunocompromised patients suffering from cancer, cystic fibrosis, drug addition, AIDS and in patients with organ transplants and on dialysis [30–32]. This organism is inherently resistant to most antibiotics due to its low outer membrane permeability [33] and to β-lactam containing antibiotics due to the production of a chromosomally expressed group 2e β-lactamase (L2) and a group 3c β-lactamase (L1) [34,35]. L1 has been cloned, over-expressed, and partially characterized by kinetic and crystallographic studies [36,37]. The enzyme exists as a homotetramer of *ca.* 118 kDa in solution and in the crystalline state. The enzyme tightly binds two Zn(II) ions per subunit and requires both Zn(II) ions for full catalytic activity. The Zn_1 site has 3 histidine residues and 1 bridging hydroxide as ligands, and the Zn_2 site has 2 histidines, 1 aspartic acid, 1 terminally-bound water, and the bridging hydroxide as ligands. Spencer and coworkers used the crystal structure and modeling studies to propose a substrate binding model and identified several active site residues that were involved in substrate binding (Figure 1) [37]. However, this model has not been tested experimentally. In order to prepare tight binding inhibitors of the metallo-β-lactamases, knowledge about how substrate binds to the enzymes is needed so that all substrate-enzyme binding contacts can be maintained in any proposed inhibitor. This work describes our efforts at understanding how substrates bind to metallo-β-lactamase L1. Several site-directed mutants of L1 were generated and characterized, and the results from these studies reveal that none of the active site residues predicted from earlier computational studies [37] are essential for tight substrate binding.

Results

Wild type L1

Wild-type L1 was over-expressed in *Escherichia coli* and purified as previously described [36]. This procedure produced an average of 50–60 mg of >90% pure, active protein per 4 L of growth culture. Circular dichroism spectra were collected on wild-type samples to ensure L1 expressed using the pET26b expression system had the correct secondary structure. The CD spectrum of wild type L1 showed an intense, broad feature at 190 nm and a smaller feature at 215 nm (see Additional file 1: CD spectra). These features are consistent with a sample with significant α/β content. The Compton and Johnson algorithm [38] was used to estimate secondary structure in the samples; wild-type L1 was estimated to have 38.3% α-helix, 26.7% β-structure (9.3% antiparallel β-sheet, 2.1% parallel β-sheet, and 15.3% β-turn), and 34.9% other structure. These estimates are in excellent agreement with the crystallographically determined secondary structure of ~40% α-helix and 30% β-structure [37]. Metal analyses on multiple preparations of wild-type L1 demonstrated that

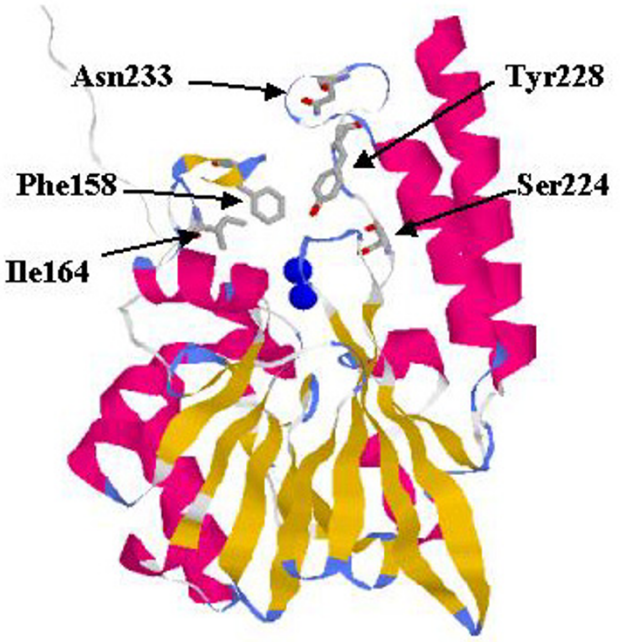

Figure 1
Active site residues that were mutated in this study. Figure was rendered using Rasmol v. 2.6. The coordinates were obtained from the Protein Data Bank using the accession number 1 sml.

the enzyme binds 1.9 ± 0.2 Zn(II) ions per monomer (Table 2), in agreement with previous results [36].

Steady state kinetic studies were performed on multiple preparations of wild type L1, and the resulting kinetic data are shown in Tables 3,4,5. When using nitrocefin as substrate and 50 mM cacodylate, pH 7.0, as buffer, wild-type L1 exhibited a k_{cat} value of 38 ± 1 s^{-1} and a K_m value of 12 ± 1 μM. The inclusion of 100 μM $ZnCl_2$ in the assay buffer resulted in slightly lower values of K_m and higher values for k_{cat}[36]. The inclusion of higher concentrations of Zn(II) did not further affect the steady-state kinetic constants. Apparently, the purified, recombinant enzyme does not bind its full complement of Zn(II); therefore, 100 μM Zn(II) was included in all subsequent kinetic studies.

Wild-type L1 exhibited k_{cat} values of 41 ± 1 s^{-1}, 1.9 ± 0.1 s^{-1}, 42 ± 1 s^{-1}, and 82 ± 5 s^{-1} for the cephalosporins, nitrocefin, cefoxitin, cefaclor, and cephalothin. For these same substrates, the K_m values were 4 ± 1 μM, 1.1 ± 0.1 μM, 13 ± 1 μM, and 8.9 ± 1.5 μM, respectively. Two penicillins were tested as substrates, and penicillin G and ampicillin exhibited K_m values of 38 ± 12 μM and 55 ± 5 μM and k_{cat} values of 600 ± 100 s^{-1} and 520 ± 10 s^{-1}, respectively (Table 4). Three carbapenems were also used as substrates for L1, and biapenem, imipenem, and meropenem exhibited K_m values of 32 ± 1 μM, 57 ± 7 μM, and 15 ± 4 μM and k_{cat} values of 134 ± 4 s^{-1}, 370 ± 5 s^{-1}, and 157 ± 9 s^{-1}, respectively (Table 5). L1's preference for penicillins and carbapenems over cephalosporins, as exemplified by the k_{cat} values, is in agreement with previous studies and supports L1's placement in the β-lactamase 3c family [9].

Rapid-scanning visible spectra of 25 μM wild-type L1 with 5 μM nitrocefin demonstrated a decrease in absorbance at 390 nm, an increase at 485 nm, and a rapid increase and slower decrease in absorbance at 665 nm. These spectra are similar to those previously reported for wild-type L1 and nitrocefin [39], and the features can be attributed to substrate decay, product formation, and intermediate formation and decay, respectively. Under these conditions, 2.2 μM intermediate was formed during the first 10 milliseconds of the reaction (Figure 2), and the rate of decay of this intermediate corresponds to the steady-state k_{cat} (Table 3). To probe further the binding of nitrocefin to wild-type L1, stopped-flow fluorescence studies were conducted as previously described [40] (Figure 3). The reaction of wild-type L1 with nitrocefin under steady-state conditions at 10°C resulted in a rapid decrease in fluorescence followed by a rate-limiting return of fluorescence (Figure 3A). Fitting of the data, as described by Spencer *et al.*[40], resulted in a K_S value for wild-type L1 of 38 ± 5 μM (Figure 3B).

Table 1: Oligonucleotides used in preparation of L1 mutants

Primer	Sequence
pUCMSZFor	CTATgCggCATCAgAgCAgATT
M13Rev	gATAACAATTTCACACAggA
Y228AFor	CTgAgTgCACCgggCgCCCAgCTgCAgggAAAC
Y228ARev	gTTTCCCTgCAgCTgggCgCCCggTgCACTCAg
Y228FFor	CTgAgTgCACCgggCTTCCAgCTgCAgggAAAC
Y228FRev	gTTTCCCTgCAgCTggAAgCCCggTgCACTCAg
S224DFor	TACgCCgACAgCCTggACgCACCgggCTACCAg
S224DRev	CAggTAgCCCggTgCgTCCAggCTgTCggCgTA
S224AFor	TACgCCgACAgCCTggCCgCACCgggCTACCAg
S224ARev	CAggTAgCCCggTgCggCCAggCTgTCggCgTA
S224KFor	TACgCCgACAgCCTgAAggCACCgggCTACCAg
S224KRev	CAggTAgCCCggTgCCTCCAggCTgTCggCgTA
F158AFor	AgCgATgACCTgCACgCCggCgATggCATCACC
F158ARev	ggTgATgCCATCgCCggCgTgCAggTCATCgCT
I164AFor	CACTTCggCgATggCgCCACCTACCCgCCTgCC
I164ARev	ggCAggCgggTAggTggCgCCATCgCCgAAgTg
N233LFor	TACCAgCTgCAgggACTgCCCCgTTATCCgCAC
N233LRev	gTgCggATAACggggCAgTCCCTgCAgCTggTA
N233DFor	TACCAgCTgCAgggAgACCCCCgTTATCCgCAC
N233DRev	gTgCggATAACgggggTCTCCCTgCAgCTggTA

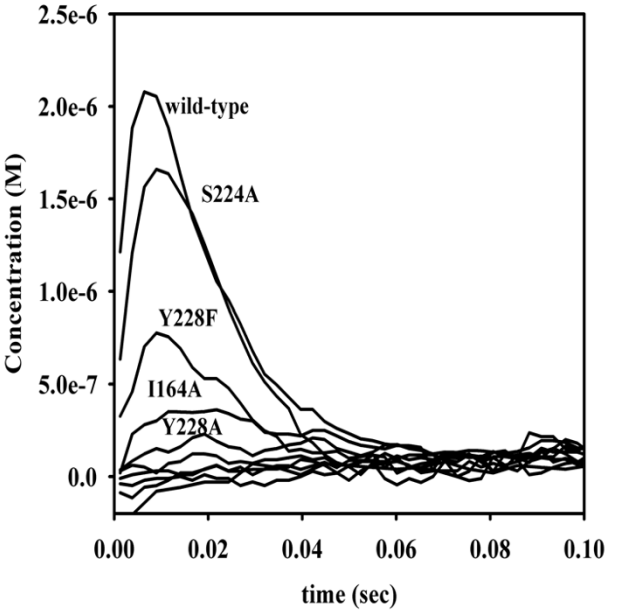

Figure 2
Intermediate formation by wild-type L1 and L1 mutants. The spectra were collected using rapid scanning Vis studies, and the absorbance values at 668 nm were converted to concentration values as described in Materials and Methods. Typical reactions were conducted with 25 μM L1 (or mutant) and 5 μM nitrocefin in 50 mM cacodylate, pH 7.0, containing 100 μM $ZnCl_2$ at 25°C.

Ser224 mutants

(the BBL numbering scheme proposed in reference 41 was used throughout this manuscript). All sequenced subclass Ba and Bb metallo-β-lactamases (except VIM-1) have a lysine residue at position 224 [41], and all computational models for substrate binding to the metallo-β-lactamases assume that the invariant carboxylate on substrates forms an electrostatic interaction with this lysine. In L1, the residue at position 224 is a serine [35], and the substrate-binding model for L1 predicts that this serine residue interacts with the carboxylate on substrate via a water molecule [37]. To test the proposed role of Ser224 in L1, serine was changed to an alanine (S224A), aspartic acid (S224D), and lysine (S224K), and these mutants were characterized using metal analyses, CD spectroscopy, steady-state kinetics, and pre-steady state kinetic studies.

Small-scale growth cultures showed that all three mutants were over-expressed at levels comparable to those of wild-type L1. Large-scale over-expression and purification of the mutants showed that all three mutants were isolatable at levels comparable to those of wild-type L1. Metal analyses of the S224A and S224D mutants showed that both mutants bind nearly two Zn(II) ions (Table 2), like wild-type L1 [36]; however, the S224K mutant binds only 1.0 Zn(II) per protein. CD spectra of the mutants were similar to those of wild-type L1 (see Figure in Additional materials). Steady-state kinetic studies were conducted with all three mutants in buffer containing 100 μM $ZnCl_2$ to ensure that both Zn(II) binding sites were saturated in these studies. Addition of higher concentrations of Zn(II) did not result in different values for the steady-state kinetic constants in Tables 3,4,5.

When the cephalosporins were used as substrates, the S224A and S224K mutants exhibited 2- to 4-fold changes in K_m values (Table 3). In studies with cefoxitin, cefaclor, and cephalothin as substrate, the observed k_{cat} values for the S224A and S224K mutants were 2- to 7-fold lower; however, the k_{cat} values when using nitrocefin as substrate were slightly higher (< 2-fold). On the other hand, the S224D mutant exhibited 3- to 50-fold higher K_m values and 2- to 20-fold lower k_{cat} values for the cephalosporins tested. A similar trend was observed in kinetic studies when using penicillins as substrates (Table 4). Generally, the S224A and S224K mutants exhibited small changes in K_m and k_{cat}, while the S224D mutant yielded 20- to 40-fold increased values for K_m and >10-fold decreases in k_{cat} when using the penicillins as substrates. When the carbapenems were used as substrates however, the changes in K_m values were relatively smaller than with the other substrates, and 2- to 37-fold changes in k_{cat} were observed (Table 5).

Rapid-scanning Vis studies of the S224X mutants were conducted to probe whether the mutations caused changes in the amount of intermediate that accumulates during catalysis. When 50 μM S224A was reacted with 5 μM ni-

Table 2: Metal Content of Wild-type L1 and L1 mutants

Sample	Zn(II) Content (moles Zn(II)/ mole of enzyme)[a]
Wild-type	1.9 ± 0.2
S224A	1.8 ± 0.2
S224D	1.7 ± 0.3
S224K	1.0 ± 0.1
Y228A	1.8 ± 0.1
Y228F	1.7 ± 0.3
F158A	1.5 ± 0.2
I164A	1.6 ± 0.2
N233L	1.8 ± 0.2
N233D	1.5 ± 0.1

[a] The final dialysis buffer was used as a blank, and the Zn(II) content in the final dialysis buffers was shown to be < 0.5 μM in separate ICP measurements.

Table 3: Steady-state kinetic constants for hydrolysis of cephalosporins by wild-type L1 and L1 mutants.

Enzyme	nitrocefin			cefoxitin			cefaclor			cephalothin		
	K_m (μM)	k_{cat} (s^{-1})	$k_{cat}/K_m \times 10^7$ M^{-1} s^{-1}	K_m (μM)	k_{cat} (s^{-1})	$k_{cat}/K_m \times 10^7$ M^{-1} s^{-1}	K_m (μM)	k_{cat} (s^{-1})	$k_{cat}/K_m \times 10^7$ M^{-1} s^{-1}	K_m (μM)	k_{cat} (s^{-1})	$k_{cat}/K_m \times 10^{-7}$ M^{-1} s^{-1}
w.t.	4 ± 1	41 ± 1	1.0	1.1 ± 0.1	1.9 ± 0.1	0.17	13 ± 1	42 ± 1	0.32	8.9 ± 1.5	82 ± 5	0.92
S224A	7 ± 1	48 ± 5	0.69	3.0 + 0.5	1.0 ± 0.1	0.033	14 ± 2	14 ± 1	0.10	3.6 ± 0.1	19.8 ± 0.2	0.55
S224K	14 ± 2	48 ± 10	0.34	2.0 ± 0.3	0.60 ± 0.06	0.030	13 ± 2	6.5 ± 0.3	0.050	6.2 ± 0.6	26 ± 1	0.42
S224D	11 ± 5	2.3 ± 0.4	0.021	50 ± 6	1.4 ± 0.2	0.0028	215 ± 17	3 ± 1	0.0014	75 ± 7	32 ± 2	0.043
I164A	8 ± 2	130 ± 30	1.6	11 ± 1	8 ± 1	0.073	3.3 + 0.5	30 ± 3	0.91	16 ± 1	146 ± 2	0.91
F158A	123 ± 20	1290 ± 20	1.0	11 ± 2	16 ± 2	0.15	135 ± 23	99 ± 9	0.073	63 ± 17	353 ± 35	0.56
Y228A	23 ± 3	72 ± 2	0.31	10 ± 2	5.8 ± 0.3	0.058	550 ± 100	40 ± 3	0.0073	290 ± 60	320 ± 40	0.11
Y228F	36 ± 16	81 ± 18	0.23	8.2 ± 1.1	5.5 ± 0.5	0.067	240 + 60	74 ± 4	0.031	58 ± 7	190 ± 50	0.33
N233L	7 ± 2	62 ± 12	0.89	4.4 ± 1.6	0.90 ± 0.17	0.020	14± 2	32 ± 1	0.23	8.0 + 0.7	51 ± 1	0.64
N233D	9 ± 2	21 ± 2	0.23	1.1 ± 0.2	1.1 ± 0.1	0.10	25 ± 5	34 ± 3	0.14	18 ± 4	65 ± 2	0.36

Table 4: Steady-state kinetic constants for hydrolysis of penicillins by wild-type L1 and L1 mutants.

Enzyme	pencilin G			ampicillin		
	K_m (μM)	k_{cat} (s^{-1})	$k_{cat}/K_m \times 10^7$	K_m (μM)	k_{cat} (s^{-1})	$k_{cat}/K_m \times 10^7$
w.t.	38 ± 12	600 ± 100	1.6	55 ± 5	520 ± 10	0.95
S224A	70 ± 20	580 ± 100	0.83	125 ± 13	339 ± 1	0.27
S224K	44 ± 8	124 ± 12	0.28	25 ± 3	152 ± 2	0.61
S224D	1600 ± 200	42 ± 9	0.0026	1100 ± 240	10 ± 1	0.00091
I164A	60 ± 5	698 ± 100	1.2	43 ± 3	524 ± 100	1.2
F158A	50 ± 5	138 ± 10	0.28	165 ± 20	270 ± 30	0.16
Y228A	410 ± 60	609 ± 64	0.15	710 ± 74	443 ± 10	0.062
Y228F	140 ± 14	630 ± 30	0.45	271 ± 40	243 ± 30	0.090
N233L	33 ± 9	184 ± 35	0.56	90 ± 20	508 ± 40	0.56
N233D	60 ± 2	440 ± 86	0.73	117 ± 18	621 ± 31	0.53

Table 5: Steady-state kinetic constants for hydrolysis of carbapenems by wild-type L1 and L1 mutants

Enzyme	biapenem			imipenem			meropenem		
	K_m (μM)	k_{cat} (s^{-1})	$k_{cat}/K_m \times 10^7$	K_m (μM)	k_{cat} (s^{-1})	$k_{cat}/K_m \times 10^7$	K_m (μM)	k_{cat} (s^{-1})	$k_{cat}/K_m \times 10^7$
w.t.	32 ± 1	134 ± 4	0.42	57 ± 7	370 ± 5	0.65	15 ± 4	157 ± 9	1.0
S224A	34 ± 5	56 ± 2	0.16	29 ± 4	100 ± 3	0.34	50 ± 10	244 ± 1	0.49
S224K	100 ± 22	43 ± 2	0.043	60 ± 4	14 ± 1	0.023	12 ± 1	212 ± 1	1.8
S224D	64 ± 7	22 ± 1	0.034	42 ± 4	17 ± 1	0.040	132 ± 23	69 ± 7	0.052
I164A	55 ± 3	112 ± 1	0.20	92 ± 11	570 ± 43	0.62	14 ± 1	96 ± 3	0.69
F158A	50 ± 11	70 ± 5	0.14	100 ± 20	370 ± 50	0.37	7 ± 2	36 ± 2	0.51
Y228A	175 ± 25	21 ± 2	0.012	350 ± 94	134 ± 36	0.038	4.5 ± 0.2	26 ± 1	0.58
Y228F	150 ± 23	51 ± 4	0.034	107 ± 13	83 ± 10	0.078	13 ± 1	70 ± 1	0.54
N233L	29 ± 3	105 ± 6	0.36	36 ± 5	250 ± 20	0.69	12 ± 1	67 ± 3	0.56
N233D	28 ± 8	7 ± 1	0.025	71 ± 16	158 ± 13	0.22	16 ± 4	3.5 ± 0.1	0.022

trocefin, 1.7 μM intermediate formed during the first 10 milliseconds of the reaction (Figure 2), and rate of decay of this intermediate was equal to the steady-state k_{cat} (Table 3). In spite of utilizing a number of reaction conditions, the S224K and S224D mutants yielded rapid-scan spectra with no detectable absorbances at 665 nm (Figure 2), indicating that the intermediate is not stabilized as well in these mutants as in wild-type L1. Stopped-flow fluorescence studies at 10°C with the S224A, S224D, and S224K mutants and nitrocefin as the substrate resulted in K_S values of 39 ± 10, 213 ± 63, and 33 ± 5 μM, respectively.

Asn233 mutants

Two-thirds of all sequenced metallo-β-lactamases have an Asn at position 233 [41], and this residue was predicted [42] and shown [43] to be involved with substrate binding and activation by interacting electrostatically with the substrate β-lactam carbonyl. However, in L1, Asn233 is 14 Å away from the modeled position of the substrate β-lactam carbonyl [37]. To test the role of Asn233 in substrate binding, the Asn was changed to a leucine (N233L) and to an aspartic acid (N233D), and these mutants were characterized by using metal analyses, CD spectroscopy, steady-state kinetics, and pre-steady state kinetic studies.

Small-scale growth cultures showed that both mutants were over-expressed at levels comparable to that of wild-type L1. Large-scale over-expression and purification of the mutants showed that both mutants were isolatable at levels comparable to that of wild-type L1. Metal analyses of the N233L and N233D mutants showed that both bind nearly two Zn(II) ions (Table 2), like wild-type L1 [36]. CD spectra of the mutants were similar to those of wild-type L1. Steady-state kinetic studies were conducted with both mutants in buffer containing 100 μM $ZnCl_2$ to ensure that both Zn(II) binding sites were saturated in these studies. Addition of higher concentrations of Zn(II) did not result in different values for the steady-state kinetic constants in Tables 3,4,5.

With all substrates tested, the N233L and N233D mutants exhibited K_m values that differed less than a factor of 4 than that observed for wild-type L1 (Tables 3,4,5). The k_{cat} values exhibited by these mutants for all substrates also differed by less than a factor of 4, except when biapenem and meropenem were used as substrates for the N233D mutant. With these two substrates, there was a 19-fold and 45-fold decrease in the k_{cat} values when using biapenem and meropenem, respectively (Table 5). The steady-state kinetic data generally support the prediction that Asn233 does not play a large role in binding or catalysis.

However, rapid-scanning Vis studies of N233L and N233D with nitrocefin demonstrate that no detectable

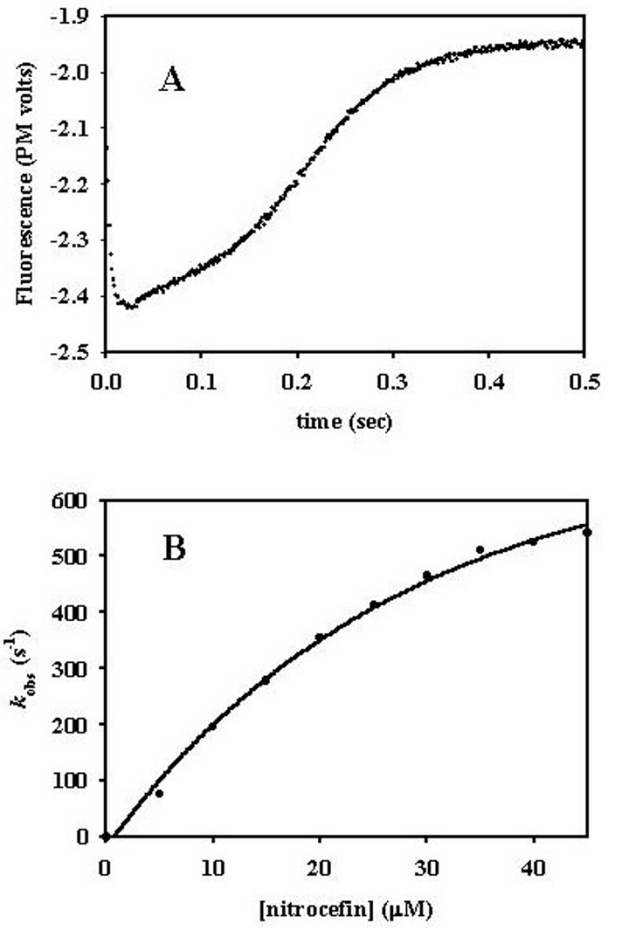

Figure 3
(A) Stopped-flow fluorescence of wild-type L1 with nitrocefin. In a typical reaction, 5–10 μM wild-type L1 was mixed with various concentrations of nitrocefin, and the reaction was monitored for up to 1 second at 10°C, using the conditions described in Materials and Methods. The data were fitted to a double exponential using SigmaPlot v. 6.10.**(B)** Plot of observed rate constant versus concentration of nitrocefin. Solid lines were fitted to the data as described in Materials and Methods.

amounts of intermediate are formed during the reaction, even when using a wide number of reaction conditions (Figure 2). Stopped-flow fluorescence studies at 10°C with the N233L and N233D mutants and nitrocefin as substrate resulted in K_S values of 26 ± 9 and 25 ± 8 μM, respectively.

Tyr228 mutants

The substrate-binding model showed that Tyr228 in L1 was position-conserved with Asn233 in the other crystallographically characterized metallo-β-lactamases [37,42,44–46]. Spencer and coworkers postulated that

Tyr228 is part of an oxyanion hole that interacts with the β-lactam carbonyl on substrate and helps to stabilize the putative tetrahedral intermediate formed during substrate turnover [37]. To test this hypothesis, Tyr228 was changed to an alanine and to a phenylalanine to afford the Y228A and Y228F mutants, respectively.

Small-scale growth cultures showed that both mutants were over-expressed at levels comparable to those of wild-type L1. Large-scale over-expression and purification of the Y228A and Y228F mutants showed that both mutants were isolatable at levels comparable to those of wild-type L1. Metal analyses of the mutants showed that both bind nearly two Zn(II) ions (Table 2), like wild-type L1 [36], and CD spectra of the mutants were similar to those of wild-type L1. Steady-state kinetic studies were conducted with both mutants in buffer containing 100 μM $ZnCl_2$ to ensure that both Zn(II) binding sites were saturated in these studies. Addition of higher concentrations of Zn(II) did not result in different values for the steady-state kinetic constants in Tables 3,4,5.

When cephalosporins were used as substrates, the Y228A and Y228F mutants exhibited K_m values that were 6- to 45-fold higher than those observed for wild-type L1 (Table 3). The largest change in K_m was observed when cefaclor was used as substrate, and the smallest change was observed when nitrocefin was used as substrate. The Tyr228 mutants exhibited < 4-fold change in k_{cat} values for the cephalosporins tested (Table 3), suggesting that Tyr228 is not playing a large role in catalysis. When penicillins were used as substrates, the Tyr228 mutants exhibited 3- to 13-fold increased K_m values and < 2-fold changes in k_{cat}, as compared to the values ascertained using wild-type L1 (Table 4). On the other hand when carbapenems were used as substrates, the Tyr228 mutants exhibited < 6-fold increases in K_m values as compared to those values for wild-type L1 (Table 5). Interestingly, there was a 2- to 8-fold drop in k_{cat} values for the Tyr228 mutants, as compared to values observed for wild-type L1, when using the carbapenems as substrates.

Rapid-scanning Vis spectra of the reaction of the Y228A and Y228F mutants with nitrocefin demonstrated a marked decrease in the amount of intermediate formed with these mutants (Figure 2). In reactions with 50 μM mutant and 5 μM nitrocefin, only 0.75 and < 0.30 μM intermediate formed for the Y228F and Y228A mutants, respectively. The concentration of mutants were varied between 25 to 150 μM to ensure that all of the substrate was bound; however, none of the reactions resulted in the detection of intermediate at levels observed for wild-type L1 (data not shown). Stopped-flow fluorescence studies at 10°C of nitrocefin hydrolysis by Y191A and Y191F resulted in K_S values of 85 ± 9 and 22 ± 6 μM, respectively.

Ile164 and Phe158 mutants

All crystallographically characterized metallo-β-lactamases have a flexible amino acid chain that extends over the active site [37,42,44–49]. Previous NMR studies on CcrA have shown that this loop "clamps down" on substrate or inhibitor upon binding, and there is speculation that the distortion of substrate upon clamping down of the loop may drive catalysis [50]. The crystal structure of L1 showed that there is a large loop that extends over the active site, and modeling studies have predicted that two residues, Ile164 and Phe158, make significant contacts with large, hydrophobic substituents at the 2' or 6' positions on penicillins, cephalosporins, or carbapenems [37]. To test this prediction, Ile 164 and Phe158 were changed from large, hydrophobic residues to alanines to afford the I164A and F158A mutants.

Small-scale growth cultures demonstrated the I164A and F158A mutants were over-expressed at levels comparable to that of wild-type L1 (data not shown). Large-scale over-expression and purification of the mutants resulted in comparable quantities of isolatable enzymes, which had identical CD spectra as wild-type L1 and bound slightly less Zn(II) than wild-type L1 (Table 2). All steady-state kinetic studies were conducted in buffers containing 100 μM $ZnCl_2$ to ensure that both metal binding sites were saturated during the studies.

When using the cephalosporins, nitrocefin, cefoxitin, and cephalothin, as substrates and the I164A mutant, there were 2- to 10-fold (only for cefoxitin) increases in K_m and 2- to 4-fold increases in k_{cat} observed (Table 3). However when cefaclor was used as substrate, the I164A mutant exhibited a 3-fold decrease in K_m and a 1.5-fold decrease in k_{cat} (Table 3). On the other hand, the K_m and k_{cat} values for the I164A mutant when the penicillins or carbapenems were used as substrates were very similar to those numbers exhibited by wild-type L1 (Tables 4 and 5).

When the cephalosporins were used as substrates for the F158A mutant, the K_m values observed were 7- to 31-fold higher than those determined for wild-type L1, and surprisingly, the k_{cat} values were 2- to 31-fold higher than those exhibited by wild-type L1 (Table 3). As with the I164A mutant, the changes in K_m and k_{cat} for the penicillins and carbapenems were relatively small, as compared with the values obtained with the cephalosporins (Table 4).

Rapid-scanning Vis studies on nitrocefin hydrolysis by I164A and F158A showed a marked decrease in intermediate accumulation, with the I164A mutant generating < 0.30 μM intermediate and the F158A producing no detectable intermediate (Figure 2). Stopped-flow fluorescence studies at 10°C resulted in a K_S value of 31 ± 11 μM for the

I164A mutant. The reaction of F158A with nitrocefin was so rapid, we could not determine a K_S value for this mutant.

Discussion

β-Lactam containing antibiotics constitute the largest class of antibiotics, and these compounds are relatively inexpensive to produce, cause minor side effects, and are effective towards a number of bacterial strains. Nonetheless, bacterial resistance to these antibiotics is extensive, most commonly due to the bacterial production of β-lactamases [10,51]. In fact, there have been over 300 distinct β-lactamases reported, and most of these enzymes utilize an active site serine group to nucleophilically attack the β-lactam carbonyl, resulting in a hydrolyzed product that is covalently attached to the active site. To combat these enzymes, β-lactamase inhibitors such as clavulanic acid, sulbactam, and tazobactam have been given in combination with a β-lactam containing antibiotic to treat bacterial infections [52]. One class of β-lactamases that are particularly unaffected by the known β-lactamase inhibitors and have been shown to hydrolyze almost all known β-lactam containing antibiotics including late generation carbapenems at high rates are the metallo-β-lactamases [14–19]. Although there are no reports of metallo-β-lactamases isolated from major pathogens [51,53], these enzymes are produced by pathogens such as *B. fragilis*, *S. maltophilia*, and *P. aeruginosa*. It is inevitable that the continued and extensive use of β-lactam antibiotics will result in a major pathogen that produces a metallo-β-lactamase.

Efforts to solve the crystal structure of one of the metallo-β-lactamases with a bound substrate molecule have failed, most likely due to the high activity of the enzymes towards all β-lactam containing antibiotics [37,54]. Therefore, computational studies have been used extensively to study substrate binding, the role of the Zn(II) ions in catalysis, the protonation state of the active site, and inhibitor binding [37,42,55–59]. All of the substrate binding models have made assumptions before the substrate was docked into the active site [37,42], and some of these assumptions have been shown to be invalid for certain substrates [43]. With L1, two key assumptions were made: (1) the bridging hydroxide functions as the nucleophile during catalysis and (2) Zn_1 coordinates the β-lactam carbonyl [37]. With these assumptions and after energy minimizations, Ser224 was predicted to hydrogen bond to the substrate carboxylate [37], reminiscent of the role predicted for Lys224 in CcrA [42]. Ullah *et al.* predicted that Phe158 and Ile 164 form hydrophobic interactions with bulky substituents on the substrate, suggesting that the loss of these residues would only affect binding of substrates with large aromatic substituents [37]. In the modeling studies on CcrA [42], Asn233 was predicted to interact with the β-lactam carbonyl on substrate, and mutagenesis studies have supported this prediction [43]. Although Asn233 is sequence conserved in L1[35], it is located 14Å away from the modeled position of the β-lactam carbonyl and was predicted not to play a role in substrate binding to L1[37]. On the other hand, the substrate-binding model predicted that Tyr228 was in position to offer a hydrogen bond to the β-lactam carbonyl and participate in an oxyanion hole that was proposed to form as the substrate was hydrolyzed [37]. By using the crystal structure and modeling studies on L1, Ullah *et al.* proposed a reaction mechanism for the enzyme [37]. To test this proposed mechanism and the proposed roles of the amino acids discussed above, site-directed mutagenesis studies were conducted on metallo-β-lactamase L1 and reported herein.

The overlap extension method [60] was used to prepare the site-directed mutants, and a variety of studies were used to probe whether the single point mutations resulted in large structural changes in the mutant enzymes. (1) The over-expression levels of mutants were analyzed with SDS-PAGE to ensure that the mutations did not result in changes in the over-expression levels of the enzymes. With a few L1 mutants and with other enzyme systems in the lab, single point mutations often result in depressed levels of over-expression [61]. In the case of the mutants described here, all of the mutants over-expressed at levels comparable to wild-type L1 (data not shown). (2) The total amounts of the mutants isolatable after chromatography were compared with wild-type L1 levels. We have found, in particular with metal binding mutants of L1 (G. Periyannan, R.B. Yates, and M.W. Crowder, unpublished results) and glyoxalase II [61], that single point mutations can result in over-expressed mutants being processed into inclusion bodies and unisolatable as soluble proteins. In the case of the mutants described here, all of the mutants were isolated at levels comparable to wild-type L1. (3) CD spectra were collected for all mutants and compared to the spectrum of wild-type L1. Although we did not expect a large change in the secondary structure of L1 upon single point mutations, CD spectroscopy is the most common structural technique to characterize site-directed mutants. All of the mutants described here exhibited CD spectra that were very similar, or identical, to that of wild-type L1 (see Additional file 1: CD spectra). (4) Metal analyses on the mutants were used to probe whether point mutations caused a significant change to the metal binding site as to preclude metal binding. The crystal structures of the metallo-β-lactamases reveal a complex and far-reaching hydrogen-bonding network around the metal binding sites, and disruption of this network is predicted to affect metal binding [37,42,44,45,48,49,62,63]. With all of the mutants described here except the S224K mutant, each mutant binds wild-type or near-wild-type levels of Zn(II) after purification. The S224K mutant exhibited a 50% re-

duction in metal binding (Table 2), and we postulate this is due to electrostatic repulsions between the newly introduced Lys with Zn_2. In spite of the mutants binding significant amounts of Zn(II), we included 100 μM $ZnCl_2$ in all of the kinetic buffers to ensure saturation of the metal binding sites and to facilitate direct comparison of the kinetic data. (5) All mutants were stable to multiple freeze/thaw cycles and to prolonged storage (> 3 weeks) at 4°C, retaining > 95% of their activity. With these five lines of evidence, we were confident that none of the point mutations resulted in large structural changes in L1 and that any kinetic differences could be attributed to the changed amino acid.

As a first approximation of substrate binding, we examined the steady-state kinetics of 4 cephalosporins, 2 penicillins, and 3 carbapenems (Tables 3,4,5) and compared the K_m values of the mutants with those of wild-type L1. The substrates tested were chosen because they exhibited low K_m values in previous kinetic studies [36], and we believed that we could saturate the enzymes with substrate even if there was large change in binding with the point mutations. The Tyr228 mutants exhibited increased K_m values for 8 of the 9 substrates tested, with the smallest changes in K_m observed when the carbapenems were used as the substrate. This result supports the proposed role of Tyr228 in substrate binding. In contrast, the results on the Ser224 mutants suggest that this residue is not important in substrate binding, since the S224A and S224K mutants did not exhibit any significant increases (by a factor of ≥ 10) in K_m for any of the substrates tested. Only when Ser224 was replaced with an Asp residue was there significant increases in the observed K_m value for 6 of the 9 substrates tested, and the largest changes were exhibited when the penicillins were used as substrates. This result supports the observation of differential binding modes of substrates to the β-lactamases, depending on the structure of the substrate [43,64,65]. The only remaining mutants that exhibited significant changes in the K_m values were the I164A and F158A mutants. The I164A mutant exhibited increased K_m values only when using cefoxitin as the substrate, suggesting an interaction of the isoleucine group with the methoxy group on cefoxitin. The F158A mutant exhibited higher K_m values when using the cephalosporins as substrates, suggesting an interaction of the cephalosporins' substituents with the phenylalanine on the loop that extends over the active site. None of the other mutants exhibited vastly different values for K_m with any of the substrates tested.

An examination of the k_{cat} values of the mutants revealed some surprising results. The S224D mutants displayed decreased k_{cat} values for 7 of the 9 substrates tested. Since similar results were not observed with the S224K and S224A mutants, we do not propose a catalytic role for Ser224. Instead, we predict that the insertion of an aspartic acid into the active site at position 224 results in a change in the hydrogen bonding network in L1; this hydrogen bonding network is extensive in all metallo-β-lactamases that have been characterized crystallographically [37,42,44,45,48,49,62,63]. The N233D mutant also exhibited greatly reduced k_{cat} values for biapenem and meropenem but not for imipenem or any of the other substrates tested. This mutation is also predicted to affect the hydrogen bonding network around the active site, and apparently, interactions of the enzyme with the 4' substituent of the carbapenems has an effect on catalysis. More surprisingly are the increases in k_{cat} of the F158A mutants. We are uncertain why the mutation of residues on the loop that extends over the active site would affect k_{cat}, since substrate and product binding have been predicted to be very fast in the reaction of nitrocefin with L1. However, we do note that the k_{cat}/K_m values of wild-type L1 and F158A differ by a factor less than 2.

The inability to propose a consistent binding model also supports the recent proposal that different substrates of L1 are hydrolyzed by different mechanisms and further suggests that using steady-state kinetic constants may not be a valid way to probe substrate binding to L1. In addition, the minimal kinetic mechanism of nitrocefin hydrolysis by L1 has been reported, and this mechanism predicts that K_m does not accurately reflect substrate binding. By using this mechanism [39], K_m is equal to $\{(k_{-1} + k_2)k_3k_4\} / \{k_1(k_3k_4 + k_2k_4 + k_2k_3\}$. To probe more directly the reaction, stopped-flow absorbance studies were conducted, and the substrate decay rates (390 nm) were studied as a function of nitrocefin concentration. While nitrocefin is a nontypical substrate, as a result of the dinitro-substituted styryl substituent [40], it is the substrate about which the most is known about its hydrolysis mechanism. Therefore, kinetic studies with nitrocefin as substrate allowed for us to evaluate the effect of point mutations on the reaction mechanism of L1. There was no clear dependence on substrate decay rates with nitrocefin concentration (data not shown). We did note though that the amount of intermediate formed during the reactions varied considerably depending upon which mutant of L1 was used in the study. All of the mutants exhibited decreases in intermediate formation, and the S224D, S224K, F158A, N233D, and N233L mutants yielded rapid-scanning data consistent with no detectable intermediate. These same mutants exhibited vastly differing K_m values. Clearly there is no correlation of K_m with the presence of the reaction intermediate. Apparently, the ability to observe the intermediate is not governed entirely by the choice of substrate [40], and it also depends on precise arrangement of active site residues. It is also possible that the site-directed mutants could be utilizing a different mechanism to hydrolyze nitrocefin [66].

Table 6: K_m and K_S values for Wild-type L1 and mutants with nitrocefin as substrate

Enzyme	K_m (μM)	K_S (μM)
Wild-type	4 ± 1	38 ± 5
S224A	7 ± 1	39 ± 10
S224D	11 ± 5	213 ± 63
S224K	14 ± 2	33 ± 5
F158A	4 ± 1	N.D.
I164A	8 ± 2	31 ± 11
Y228A	23 ± 3	85 ± 9
Y228F	36 ± 16	22 ± 6
N233D	9 ± 2	26 ± 8
N233L	7 ± 2	25 ± 7

N.D. – not determined

Recently, Spencer and co-workers reported that stopped-flow fluorescence studies can be used to monitor the reaction of L1 with nitrocefin and that an initial binding step can be directly monitored [40]. By increasing the concentration of nitrocefin, the rate of the initial binding step increased to a maximum, and fitting of these data yielded a binding constant (called K_S herein) for nitrocefin. Each of the L1 mutants were studied using the stopped-flow fluorescence studies, and the resulting data were fitted as reported by Spencer *et al.*[40] (Table 6). All of the mutants exhibited K_S values identical, within error, to wild-type L1, except the S224D and the Y228A mutants. The placement of a negative charge at position 224 drastically affects nitrocefin binding and results in a 6-fold decrease in binding affinity (Table 6). To a lesser degree, the aromatic portion of Tyr228 must have an effect on the binding site as the K_S value for nitrocefin binding to this mutant is decreased by a factor of 2; however, the hydroxyl group probably does not form a hydrogen bond to the substrate as proposed. By using nitrocefin as substrate and K_m values alone, a completely different conclusion is reached regarding important substrate binding residues. The results presented here suggests that none of the residues in this study are essential for tight nitrocefin binding, possibly because other parts of the active site accommodate the loss of certain binding contacts.

Spencer *et al.* also reported stopped-flow fluorescence studies when using cefaclor and meropenem as substrates, and K_S values for these substrates were reported to be 710 ± 180 and 272 ± 112 μM, respectively [40]. However in our hands, the rates of substrate hydrolysis were so fast when using wild-type L1 that we could not use substrate concentrations high enough to saturate the enzyme. Similarly, we could not determine K_S values for penicillin G or ampicillin because the observed rates of hydrolysis at low substrate concentrations were too fast to observe data, even at 10°C.

Conclusions

The results presented herein indicate that none of the active site residues identified with computational studies are essential for tight substrate binding. These data also indicate that the use of K_m values to describe substrate binding to L1 is unreliable and that there is no correlation between intermediate accumulation and substrate binding affinity. These results demonstrate that new computational studies are now needed to probe substrate binding to L1, and these studies are currently underway. The results presented herein can be used to guide these new computational studies, which will lead to the design of potential inhibitors and hopefully a way to combat penicillin resistance in bacteria.

Materials and Methods

Materials

E. coli strains DH5α and BL21(DE3) pLysS were obtained from Gibco BRL and Novagen, respectively. Plasmids pET26b and pUC19 were purchased from Novagen. Primers for sequencing and mutagenesis studies were purchased from Integrated DNA Technologies. Deoxynucleotide triphosphates (dNTP's), $MgSO_4$, thermopol buffer, Deep Vent DNA polymerase, and restrictions enzymes were purchased from Promega or New England Biolabs. Polymerase chain reaction was conducted using a Thermolyne Amplitron II unit. DNA was purified using the Qiagen QIAQuick gel extraction kit or Plasmid Purification kit with QIAGEN-tip 100 (Midi) columns. Wizard Plus Minipreps were acquired from Promega. Luria-Bertani (LB) media was made following published procedures [67]. Isopropyl-β-thiogalactoside (IPTG), Biotech grade, was procured from Anatrace. Phenylmethylsulfonylfluoride (PMSF) was purchased from Sigma. Protein solutions were concentrated with an Amicon ultrafiltration cell equipped with YM-10 DIAFLO membranes from Amicon, Inc. Dialysis tubing was prepared using Spectra/Por regenerated cellulose molecular porous membranes with a molecular weight cut-off of 6–8,000 g/mol. Q-Sepharose Fast Flow was purchased from Amersham Pharmacia Biotech. Nitrocefin was purchased from Becton Dickinson, and solutions of nitrocefin were filtered through a Fisherbrand 0.45 micron syringe filter. Cefaclor, cefoxitin, and cephalothin were purchased from Sigma; penicillin G and ampicillin were purchased from Fisher. Imipenem, meropenem, and biapenem were generously supplied by Merck, Zeneca Pharmaceuticals, and Lederle (Japan), respectively. All buffers and media were prepared using Barnstead NANOpure ultrapure water.

Generation of site-directed mutants of L1

The over-expression plasmid for L1, pUB5832, was digested with *Nde*I and *Hind*III, and the resulting *ca.* 900 bp piece was gel purified and ligated using T4 ligase into pUC19, which was also digested with *Nde*I and *Hind*III, to yield the cloning plasmid pL1PUC19. Mutations were introduced into the L1 gene by using the overlap extension method of Ho *et al.*[60], as described previously [68]. The oligonucleotides used for the preparation of the mutants are shown in Table 1. The *ca.* 900 bp PCR products were digested with *Nde*I and *Hind*III and ligated into pUC19. The DNA sequences were analyzed by the Biosynthesis and Sequencing Facility in the Department of Biological Chemistry at Johns Hopkins University. After confirmation of the sequence, the mutated pL1PUC19 plasmid was digested with *Nde*I and *Hind*III, and the 900 bp, mutated L1 gene was gel purified and ligated into pET26b to create the mutant overexpression plasmids. To test for overexpression of the mutant enzymes, *E. coli* BL21(DE3)pLysS cells were transformed with the mutated over-expression plasmids, and small scale growth cultures were used [68]. Large-scale (4 L) preparations of the L1 mutants were performed as described previously [36]. Protein purity was ascertained by SDS-PAGE.

Metal content

The concentrations of L1 and the mutants were determined by measuring the proteins' absorbance at 280 nm and using the published extinction coefficient of ε_{280} nm = 54,804 $M^{-1}\bullet cm^{-1}$[36] or by using the method of Pace [69]. Before metal analyses, the protein samples were dialyzed versus 3 × 1 L of metal-free, 50 mM HEPES, pH 7.5 over 96 hours at 4°C. A Varian Inductively Coupled Plasma Spectrometer with atomic emission spectroscopy detection (ICP-AES) was used to determine metal content of multiple preparations of wild type L1 and L1 mutants. Calibration curves were based on three standards and had correlation coefficient limits of at least 0.9950. The final dialysis buffer was used as a blank, and the Zn(II) content in the final dialysis buffers was shown to be < 0.5 μM (detection limit of ICP) in separate ICP measurements. The emission line of 213.856 nm is the most intense for zinc and was used to determine the Zn content in the samples. The errors in metal content data reflect the standard deviation (σ_{n-1}) of multiple enzyme preparations.

Steady-state kinetic studies

Steady-state kinetic assays were conducted at 25°C in 50 mM cacodylate buffer, pH 7.0, containing 100 μM $ZnCl_2$ on a HP 5480A diode array UV-Vis spectrophotometer at 25°C. The changes in molar absorptivities (Δε) used to quantitate products were (in $M^{-1}cm^{-1}$): nitrocefin, $\Delta\varepsilon_{485}$ = 17,420; cephalothin, $\Delta\varepsilon_{265}$= -8,790; cefoxitin, $\Delta\varepsilon_{265}$= -7,000; cefaclor, $\Delta\varepsilon_{280}$= -6,410; imipenem, $\Delta\varepsilon_{300}$= -9,000; meropenem, $\Delta\varepsilon_{293}$= -7,600; biapenem, $\Delta\varepsilon_{293}$= -8,630; ampicillin, $\Delta\varepsilon_{235}$= -809; and penicillin G, $\Delta\varepsilon_{235}$ = -936. When possible, substrate concentrations were varied between 0.1 to 10 times the K_m value. In kinetic studies using substrates with low K_m values (cefoxitin, nitrocefin, and cephalothin) or with small Δε values (penicillin and ampicillin), we typically used substrate concentrations varied between ~ K_m and 10 × K_m and used as much of the ΔA versus time data (that was linear) as possible to determine the velocity. Steady-state kinetics constants, K_m and k_{cat}, were determined by fitting initial velocity versus substrate concentration data directly to the Michaelis equation using CurveFit [36]. The reported errors reflect fitting uncertainties. All steady-state kinetic studies were performed in triplicate with recombinant L1 from at least three different enzyme preparations.

Circular dichroism

Circular dichroism samples were prepared by dialyzing the purified enzyme samples versus 3 × 2 L of 5 mM phosphate buffer, pH 7.0 over six hours. The samples were diluted with final dialysis buffer to ~75 μg/mL. A JASCO J-810 CD spectropolarimeter operating at 25°C was used to collect CD spectra.

Stopped – flow/Rapid-Scanning UV-Visible Spectrophotometry

Rapid-scanning Vis spectra of nitrocefin hydrolysis by L1 and the L1 mutants were collected on a Applied Photophysics SX.18MV stopped-flow spectrophotometer equipped with an Applied Photophysics PD.l photodiode array detector and a 1 cm pathlength optical cell. A typical experiment consisted of 25 μM enzyme and 5 μM nitrocefin in 50 mM cacodylate buffer, pH 7.0 containing 100 μM $ZnCl_2$, the reaction temperature was thermostated at 25°C, and the spectra were collected between 300 and 725 nm. Data from at least three experiments were collected and averaged. Absorbance data were converted to concentration data as described previously by McMannus and Crowder [39]. Stopped-flow fluorescence studies of nitrocefin hydrolysis by L1 were performed on an Applied Photophysics SX.18MV spectrophotometer, using an excitation wavelength of 295 nm and a WG320 nm cut-off filter on the photomultiplier. These experiments were conducted at 10°C using the same buffer in the rapid-scanning Vis studies. Fluorescence data were fitted to $k_{obs} = \{(k_f [S]) / K_S + [S])\} + k_r$ as described previously [40] or to $k_{obs} = k_f [S] + k_r$ by using CurveFit v. 1.0.

Abbreviations

AES, atomic emission spectroscopy; bp, base pairs; CD, circular dichroism; ε, extinction coefficient; ICP, inductively coupled plasma; k_{cat}, turnover number; kDa, kilodaltons; K_m, Michaelis constant; K_S, substrate binding constant; LB, Luria-Bertani media.

Additional material

Additional file 1

The data were collected at 25 ℃ on a JASCO J-810 CD Spectropolarimeter. The enzymes were dialyzed into 5 mM phosphate buffer, pH 7.0, and were 75 μg/mL.

CD spectra of wild-type L1 and mutants
[http://www.biomedcentral.com/content/supplementary/1471-2091-3-4-S1.jpeg]

Acknowledgements

The authors acknowledge NIH R29 AI40052 (to M.W.C) for funding this work, NSF DBI-0070169 for funding the CD spectropolarimeter, and NSF CHE-0076936 for funding the stopped-flow UV-Vis spectrophotometer used in these studies. RBY was a recipient of a 2001 Miami University Summer Scholars award. The authors would like to thank Drs. James Spencer and Tim Walsh for helpful conversations.

References

1. Matagne A, Dubus A, Galleni M, Frere JM: **The β-Lactamase Cycle: A Tale of Selective Pressure and Bacterial Ingenuity.** *Nat. Prod. Rep.* 1999, **16:**1-19
2. Wright GD: **Resisting Resistance: New Chemical Strategies for Battling Superbugs.** *Chem. & Biol.* 2000, **7:**R127-R132
3. Levy SB: **The Challenge of Antibiotic Resistance.** *Scient. Amer.* 1998, **3:**47-53
4. Kotra LP, Mobashery S: **Mechanistic and Clinical Aspects of β-Lactam Antibiotics and β-Lactamases.** *Arch. Immunol. Ther. Exp.* 1999, **47:**211-216
5. Bush K, Mobashery S: **How β-Lactamases Have Driven Pharmaceutical Drug Discovery.** *Adv. Exp. Med. Biol.* 1998, **456:**71-98
6. Page MI: **The Mechanisms of Reactions of β-Lactam Antibiotics.** *Acc. Chem. Res.* 1984, **17:**144-151
7. Knowles JR: **Penicillin Resistance: The Chemistry of β-Lactamase Inhibition.** *Acc. Chem. Res.* 1985, **18:**97-104
8. Ambler RP: **The Structure of β-Lactamases.** *Phil. Trans. Royal Soc. London B* 1980, **289:**321-331
9. Bush K: **Metallo-β-Lactamases: A Class Apart.** *Clin. Infect. Dis.* 1998, **27(Supplement 1):**48-53
10. Bush K, Jacoby GA, Medeiros AA: **A Functional Classification Scheme for β-lactmases and Its Correlation with Molecular Structure.** *Antimicro. Agents Chemo.* 1995, **39:**1211-1233
11. Bush K: **Characterization of β-Lactamases.** *Antimicro. Agents Chemo.* 1989, **33:**259-263
12. Bush K: **Classification of β-lactmases: Groups 1, 2a, 2b, and 2b'.** *Antimicro. Agents Chemo.* 1989, **33:**264-270
13. Bush K: **Classification of β-lactmases: Groups 2c, 2d, 2e, 3 and 4.** *Antimicro. Agents Chemo.* 1989, **33:**271-276
14. Payne DJ: **Metallo-β-lactamases – A New Therapeutic Challenge.** *J. Med. Microbiol.* 1993, **39:**93-99
15. Rasmussen BA, Bush K: **Carbapenem-Hydrolyzing β-Lactamases.** *Antimicro. Agents Chemo.* 1997, **41:**223-232
16. Cricco JA, Orellano EG, Rasia RM, Ceccarelli EA, Vila AJ: **Metallo-β-Lactamases: Does it Take Two to Tango?** *Coord. Chem. Rev.* 1999, **190-192:**519-535
17. Cricco JA, Vila AJ: **Class B β-Lactamases: the Importance of Being Metallic.** *Curr. Pharma. Des.* 1999, **5:**915-927
18. Crowder MW, Walsh TR: **Metallo-β-Lactamases: Structure and Function.** *Research Signpost* 1999, **3:**105-132
19. Wang Z, Fast W, Valentine AM, Benkovic SJ: **Metallo-β-Lactamases: Structure and Mechanism.** *Curr. Opin. Chem. Biol.* 1999, **3:**614-622
20. Payne DJ, Bateson JH, Gasson BC, Proctor D, Khushi T, Farmer TH, Tolson DA, Bell D, Skett PW, Marshall AC, Reid R, Ghosez L, Combret Y, Marchand-Brynaert J: **Inhibition of Metallo-β-Lactamases by a Series of Mercaptoacetic Acid Thiol Ester Derivatives.** *Antimicro. Agents Chemo.* 1997, **41:**135-140
21. Payne DJ, Bateson JH, Gasson BC, Khushi T, Proctor D, Pearson SC, Reid R: **Inhibition of Metallo-β-Lactamases by a Series of Thiol Ester Derivatives of Mercaptophenylacetic Acid.** *FEMS Micro. Lett.* 1997, **157:**171-175
22. Yang KW, Crowder MW: **Inhibition Studies on the Metallo-β-Lactamase L1 from *Stenotrophomonas maltophilia*.** *Arch. Biochem. Biophys.* 1999, **368:**1-6
23. Felici A, Perilli M, Segatore B, Franceschini N, Setacci D, Oratore A, Stefani S, Galleni M, Amicosante G: **Interactions of Biapenem with Active Site Serine and Metallo-β-Lactamases.** *Antimicro. Agents Chemo.* 1995, **39:**1300-1305
24. Gilpin ML, Fulston M, Payne D, Cramp R, Hood I: **Isolation and Structure Determination of Two Novel Phenazines from a *Streptomyces* with Inhibitory Activity against Metallo-enzymes, Including Metallo-β-Lactamase.** *J. Antibiotics* 1995, **48:**1081-1085
25. Prosperi-Meys C, Llabres G, de Seny D, Soto RP, Valladares MH, Laraki N, Frere JM, Galleni M: **Interaction between Class B β-Lactamases and Suicide Substrates of Active-Site Serine β-Lactamases.** *FEBS Letters* 1999, **443:**109-111
26. Nagano R, Adachi Y, Imamura H, Yamada K, Hashizume T, Morishima H: **Carbapenem Derivatives as Potential Inhibitors of Various β-Lacamases, Including Class B Metallo-β-Lactamases.** *Antimicro. Agents Chemo.* 1999, **43:**2497-2503
27. Toney JH, Cleary KA, Hammond GG, Yuan X, May WJ, Hutchins SM, Ashton WT, Vanderwall DE: **Structure-Activity Relationships of Biphenyl Tetrazoles as Metallo-β-Lactamase Inhibitors.** *Bioorg. Med. Chem. Lett.* 1999, **9:**2741-2746
28. Arakawa Y, Shibata N, Shibayama K, Kurokawa H, Yagi T, Fujiwara H, Goto M: **Convenient Test for Screening Metallo-β-Lactamase Producing Gram Negative Bacteria by Using Thiol Compounds.** *J. Clin. Microbiol.* 2000, **38:**40-43
29. Payne DJ, Du W, Bateson JH: **β-Lactamase Epidemiology and the Utility of Established and Novel β-Lactamase Inhibitors.** *Exp. Opin. Invest. Drugs* 2000, **9:**247-261
30. Khardori N, Elting L, Wong E, Schable B, Bodey GP: **Nosocomial Infections Due to *Xanthomonas maltophilia* in Patients with Cancer.** *Rev. Infect. Dis.* 1990, **12:**997-1003
31. Muder RR, Yu VL, Dummer JS, Vinson C, Lumish RM: **Infections Caused by *Pseudomonas maltophilia*.** *Arch. Internal Med.* 1987, **147:**1672-1674
32. Villarino ME, Stevens LE, Schable B, Mayers G, Miller JM, Burke JP, Jarvis WR: **Risk Factors for Epidemic *Xanthomonas maltophilia* Infection/Colonization in Intensive Care Unit Patients.** *Infection Control and Hospital Epidemiology* 1992, **13:**201-206
33. Mett H, Rosta S, Schacher B, Frei R: **Outer Membrane Permeability and β-lactamase Content in *Pseudomonas maltophilia* Clinical Isolates and Laboratory Mutants.** *Rev. Infect. Dis.* 1988, **10:**765-819
34. Walsh TR, Payne DJ, Neville T, Tolson D, MacGowan AP, Bennett PM: **Sequence Analysis and Kinetics of the Cloned L2 Serine β-Lactamase from *Stenotrophomonas maltophilia*.** *Antimicro. Agents Chemo.* 1997, **41:**1460-1462
35. Walsh TR, Hall L, Assinder SJ, Nichols WW, Cartwright SJ, MacGowan AP, Bennett PM: **Sequence Analysis of the L1 Metallo-β-Lactamase from *Xanthomonas maltophilia*. *Biochim.*** *Biophys. Acta* 1994, **1218:**199-201
36. Crowder MW, Walsh TR, Banovic L, Pettit M, Spencer J: **Overexpression, Purification, and Characterization of the Cloned Metallo-β-Lactamase L1 from *Stenotrophomonas maltophilia*.** *Antimicro. Agents Chemo.* 1998, **42:**921-926
37. Ullah JH, Walsh TR, Taylor IA, Emery DC, Verma CS, Gamblin SJ, Spencer J: **The Crystal Structure of the L1 Metallo-β-Lactamase from *Stenotrophomonas maltophilia* at 1.7 A Resolution.** *J. Mol. Biol.* 1998, **284:**125-136
38. Compton LA, Johnson WC: **Analysis of Protein Circular Dichroism Spectra for Secondary Structure Using a Simple Matrix Multiplication.** *Anal. Chem.* 1986, **155:**155-167
39. McMannus-Munoz S, Crowder MW: **Kinetic Mechanism of Metallo-β-Lactamase L1 from *Stenotrophomonas maltophilia*.** *Biochemistry* 1999, **38:**1547-1553
40. Spencer J, Clark AR, Walsh TR: **Novel Mechanism of Hydrolysis of Therapeutic β-Lactams by *Stenotrophomonas maltophilia* L1 Metallo-β-Lactamase.** *J. Biol. Chem.* 2001, **276:**33638-33644

41. Galleni M, Lamotte-Brasseur J, Rossolini GM, Spencer J, Dideberg O, Frere JM: **Standard Numbering Scheme for Class B β-Lactamases.** *Antimicro. Agents Chemo.* 2001, **45:**660-663
42. Concha NO, Rasmussen BA, Bush K, Herzberg O: **Crystal Structure of the Wide-Spectrum Binuclear Zinc β-Lactamase from *Bacteroides fragilis.*** *Structure* 1996, **4:**823-836
43. Yanchak MP, Taylor RA, Crowder MW: **Mutational Analysis of Metallo-β-Lactamase CcrA from *Bacteroides fragilis.*** *Biochemistry* 2000, **39:**11330-11339
44. Carfi A, Duee E, Galleni M, Frere JM, Dideberg O: **1.85 A Resolution Structure of the ZincII β-Lactamase II from *Bacillus cereus.*** *Acta Cryst.* 1998, **54:**D313-323
45. Concha NO, Janson CA, Rowling P, Pearson S, Cheever CA, Clarke BP, Lewis C, Galleni M, Frere JM, Payne DJ, Bateson JH, Abdel-Meguid SS: **Crystal Structure of the IMP-1 Metallo-β-Lactamase from *Pseudomonas aeruginosa* and Its Complex with a Mercaptocarboxylate Inhibitor: Binding Determinants of a Potent, Broad-Spectrum Inhibitor.** *Biochemistry* 2000, **39:**4288-4298
46. Fabiane SM, Sohi MK, Wan T, Payne DJ, Bateson JH, Mitchell T, Sutton BJ: **Crystal Structure of the Zinc-Dependent β-Lactamase from *Bacillus cereus* at 1.9 A Resolution: Binuclear Active Site with Features of a Mononuclear Enzyme.** *Biochemistry* 1998, **37:**12404-12411
47. Carfi A, Pares S, Duee E, Galleni M, Duez C, Frere JM, Dideberg O: **The 3-D Structure of a Zinc Metallo-β-Lactamase from *Bacillus cereus* Reveals a New Type of Protein** *Fold. EMBO J.* 1995, **14:**4914-4921
48. Concha NO, Rasmussen BA, Bush K, Herzberg O: **Crystal Structures of the Cadmium- and Mercury-Substituted Metallo-β-Lactamase from textitBacteroides fragilis** . *Prot. Sci.* 1997, **6:**2671-2676
49. Fitzgerald PMD, Wu JK, Toney JH: **Unanticipated Inhibition of the Metallo-β-Lactamase from *Bacteroides fragilis* by 4-Morpholineethanesulfonic Acid (MES): A Crystallographic Study at 1.85 A Resolution.** *Biochemistry* 1998, **37:**6791-6800
50. Scrofani SDB, Chung J, Huntley JJA, Benkovic SJ, Wright PE, Dyson HJ: **NMR Characterization of the Metallo-β-lactamase from *Bacteroides fragilis* and Its Interaction with a Tight-Binding Inhibitor: Role of an Active-Site Loop.** *Biochemistry* 1999, **38:**14507-14514
51. Bush K: **β-Lactamases in Gram-Negative Bacteria: Diversity and Impact on the Selection of Antimicrobial Therapy.** *Clin. Infect. Dis.* 2001, **32:**New1085-1090
52. Williams JD: **β-Lactamases and β-Lactamase Inhibitors.** *Int. J. Antimicro. Agents* 1999, **12 Supplement 1:**S3-S7
53. Rice LB, Bonomo RA: **β-Lactamases: Which Ones are Clinically Important?** *Drug Resist. Updates* 2000, **3:**178-189
54. Carfi A, Paul-Soto R, Martin L, Petillot Y, Frere JM, Dideberg O: **Purification, Crystallization, and Preliminary X-Ray Analysis of *Bacteroides fragilis* Zn^{2+} β-Lactamase.** *Acta Cryst.* 1997, **D53:**485-487
55. Bernstein NJ, Pratt RF: **On the Importance of a Methyl Group in β-Lactamase Evolution: Free Energy Profiles and Molecular Modeling.** *Biochemistry* 1999, **38:**10499-10510
56. Diaz N, Suarez D, Merz KM: **Zinc Metallo-β-Lactamase from *Bacteroides fragilis:* A Quantum Chemical Study on Model Systems of the Active Site.** *J. Am. Chem. Soc.* 2000, **122:**4197-4208
57. Caselli E, Powers RA, Blaszczak LC, Wu CYE, Prati F, Shoichet BK: **Energetic, Structural, and Antimicrobial Analyses of β-Lactam Side Chain Recognition by β-Lactamases.** *Chem. & Biol.* 2000, **49:**1-16
58. Suarez D, Merz KM: **Molecular Dynamics Simulations of the Mononuclear Zinc-β-Lactamase from *Bacillus cereus.*** *J. Am. Chem. Soc.* 2001, **123:**3759-3770
59. Salsbury FR, Crowley MF, Brooks CL: **Modeling of the metallo-beta-lactamase from *B. fragilis:* Structural and dynamic effects of inhibitor binding.** *Proteins-Structure Function and Genetics* 2001, **44:**448-459
60. Ho SN, Hunt HD, Horton RM, Pullen JK, Pease LR: **Site-Directed Mutagenesis by Overlap Extension Using the Polymerase Chain Reaction.** *Gene* 1989, **77:**51-59
61. Zang TM, Hollman DA, Crawford PA, Crowder MW, Makaroff CA: ***Arabidopsis* Glyoxalase II Contains a Zinc/Iron Binuclear Metal Center That Is Essential for Substrate Binding and Catalysis.** *J. Biol. Chem.* 2001, **276:**4788-4795
62. Toney JH, Hammond GG, Fitzgerald PMD, Sharma N, Balkovec JM, Rouen GP, Olson SH, Hammond ML, Greenlee ML, Gao Y-D: **Succinic Acids as Potent Inhibitors of Plasmid-borne IMP-1 Metallo-beta-lactamase.** *J. Biol. Chem.* 2001, **276:**31913-31501
63. Toney JH, Fitzgerald PMD, Grover-Sharma N, Olson SH, May WJ, Sundelof JG, Vanderwall DE, Cleary KA, Grant SK, Wu JK, Kozarich JW, Pompliano DL, Hammond GG: **Antibiotic Sensitization Using Biphenyl Tetrazoles as Potent Inhibitors of *Bacteroides fragilis* Metallo-β-Lactamase.** *Chem. & Biol.* 1998, **5:**185-196
64. Zafaralla G, Manavathu EK, Lerner SA, Mobashery S: **Elucidation of the Role of Arginine-244 in the Turnover Processes of Class A β-Lactamases.** *Biochemistry* 1992, **31:**3847-3852
65. Imtiaz U, Manavathu EK, Lerner SA, Mobashery S: **Critical Hydrogen Bonding by Serine 235 for Cephalosporinase Activity of TEM-1 β-Lactamase.** *Antimicro. Agents Chemo.* 1993, **37:**2438-2442
66. Peracchi A: **Enzyme catalysis: removing chemically 'essential' residues by site-directed mutagenesis.** *Trends Biochem. Sci.* 2001, **26:**497-503
67. Sambrook J, Fritsch EF, Maniatis T: *Molecular Cloning – A Laboratory Manual* 1989
68. Crowder MW, Yang KW, Carenbauer AL, Periyannan G, Seifert MA, Rude NE, Walsh TR: **The Problem of a Solvent Exposable Disulfide when Preparing Co(II)-Substituted Metallo-β-Lactamase L1 from *Stenotrophomonas maltophilia.*** *J. Biol. Inorg. Chem.* 2001, **6:**91-99
69. Pace CN, Vajdos F, Fee L, Grimsley G, Gray T: **How to Measure and Predict the Molar Absorption Coefficient of a Protein.** *Prot. Sci.* 1995, **4:**2411-2423